A Functional Role for Antibodies in Tuberculosis

Citation: Lu, Lenette L. et al. "A Functional Role for Antibodies in Tuberculosis." Cell 167, 2 (October 2016): 433–443 © 2016 Elsevier Inc

As Published: http://dx.doi.org/10.1016/J.CELL.2016.08.072

Publisher: Elsevier

Persistent URL: http://hdl.handle.net/1721.1/117692

Version: Final published version: final published article, as it appeared in a journal, conference proceedings, or other formally published context

HHS Public Access

Author manuscript

Cell. Author manuscript; available in PMC 2017 October 06.

Published in final edited form as:

Cell. 2016 October 06; 167(2): 433–443.e14. doi:10.1016/j.cell.2016.08.072.

A functional role for antibodies in tuberculosis

Lenette L. Lu[1,2,*], **Amy W. Chung**[1,3,*], **Tracy Rosebrock**[2,*], **Musie Ghebremichael**[1], **Wen Han Yu**[1,4], **Patricia S. Grace**[1], **Matthew K. Schoen**[1], **Fikadu Tafesse**[1], **Constance Martin**[2], **Vivian Leung**[2], **Alison E. Mahan**[1], **Magdalena Sips**[1,6], **Manu Kumar**[4], **Jacquelynne Tedesco**[1], **Hannah Robinson**[1], **Elizabeth Tkachenko**[1], **Monia Draghi**[1], **Katherine J. Freedberg**[1], **Hendrik Streeck**[5], **Todd J. Suscovich**[1], **Douglas Lauffenburger**[4], **Blanca I. Restrepo**[7], **Cheryl Day**[8,9], **Sarah M. Fortune**[2,*], and **Galit Alter**[1,*]

[1]Ragon Institute of MGH, MIT, and Harvard, Cambridge, MA, 02139, USA

[2]Department of Immunology and Infectious Diseases, Harvard School of Public Health, Boston, MA, 02115, USA

[3]Department of Microbiology and Immunology, University of Melbourne, Doherty Institute for Infection and Immunity, Melbourne, 3000, Australia

[4]Department of Biological Engineering, Massachusetts Institute of Technology, Cambridge, MA, 02142, USA

[5]Duisburg-Essen University, Essen, Germany

[6]Department of Biomedical Molecular Biology, Ghent University, Ghent, 9000, Belgium

[7]School of Public Health, University of Texas Health Houston, Brownsville, TX, 78520, USA

[8]Emory Vaccine Center, Emory University School of Medicine, Atlanta, GA Department of Microbiology and Immunology, Emory University School of Medicine, Atlanta, GA, 30332, USA

[9]South African Tuberculosis Vaccine Initiative (SATVI) and School of Child and Adolescent Health, Institute of Infectious Diseases and Molecular Medicine, University of Cape Town, Observatory 7925 South Africa

Summary

While a third of the world carries the burden of tuberculosis, disease control has been hindered by the lack of tools including a rapid, point-of-care diagnostic and a protective vaccine. In many infectious diseases, antibodies (Abs) are powerful biomarkers and important immune mediators. However, in *Mycobacterium tuberculosis* (Mtb) infection, a discriminatory or protective role for humoral immunity remains unclear. Using an unbiased antibody profiling approach we show that

Corresponding author and lead contact: Galit Alter, galter@mgh.harvard.edu, Ragon Institute of MGH, MIT, and Harvard University, Harvard Medical School, 400 Technology Square, Cambridge, MA 02139, 857-268-7003. Corresponding author: Sarah M. Fortune, sfortune@hsph.harvard.edu, Harvard School of Public Health, Ragon Institute of MGH, MIT, and Harvard University, 665 Huntington Avenue, Boston, MA 02115, 617-432-3337.

*These authors contributed equally to this work

individuals with latent tuberculosis infection (Ltb) and active tuberculosis disease (Atb) have distinct Mtb-specific humoral responses, such that Ltb infection is associated with unique Ab Fc functional profiles, selective binding to FcγRIII, and distinct Ab glycosylation patterns. Moreover, compared to Abs from Atb, Abs from Ltb drove enhanced phagolysosomal maturation, inflammasome activation, and most importantly, macrophage killing of intracellular Mtb. Combined, these data point to a potential role for Fc-mediated Ab effector functions, tuned via differential glycosylation, in Mtb control.

Graphical abstract

Individuals with active and latent tuberculosis infections can be distinguished by the type of antibodies they produce, pointing toward an important and unappreciated contribution from humoral immunity in controlling chronic TB.

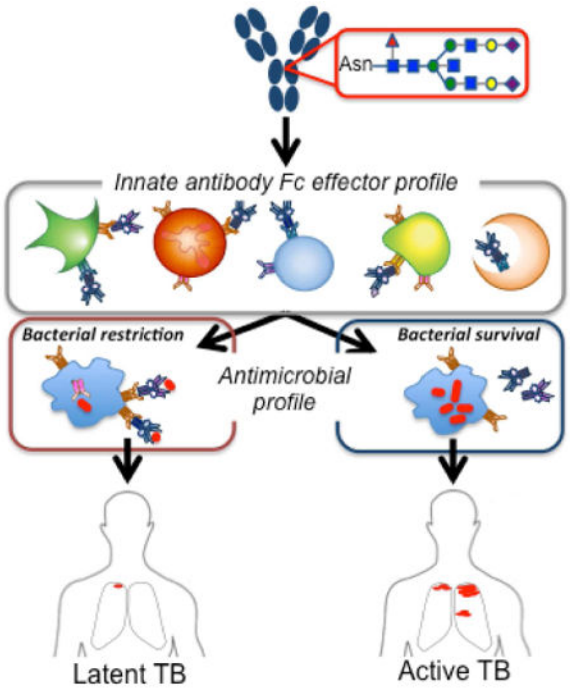

Introduction

Despite the high global burden of *Mycobacterium tuberculosis* (Mtb) infection (Zumla et al., 2013), the immunological mechanism(s) underlying bacterial control remains unclear (O'Garra et al., 2013). While cellular immunity is important, the role of humoral immunity in tuberculosis (TB) is uncertain (Achkar et al., 2015; Kozakiewicz et al., 2013). Complement opsonization does not affect Mtb survival (Zimmerli et al., 1996), higher antibody (Ab) titers correlate with disease severity (Doherty et al., 2009; Steingart et al., 2011), and passive transfer of Abs have inconsistently conferred protection (Balu et al., 2011; Hamasur et al., 2004; Suter, 1953; Teitelbaum et al., 1998). However, Abs, plasma cells, and Ab-responsive innate immune cells bearing Fc receptors (FcR) are abundant in TB granulomas (Phuah et al., 2012; Tsai et al., 2006), suggesting that they may play a role in the

antimicrobial response. Along these lines, Abs against the Mtb lipoarabinomannan enhance bacterial opsonization and restrict intracellular growth (Chen et al., 2016; de Valliere et al., 2005). Moreover, while B cell and Ab deficiencies are not risk factors for TB disease (Glatman-Freedman and Casadevall, 1998), mice lacking B cells or the ability to secrete Abs are more susceptible to infection (Maglione et al., 2007; Torrado et al., 2013; Vordermeier et al., 1996), and depletion of B cells in non-human primates (NHPs) results in increased lesional bacterial burden (Phuah et al., 2016). Finally, elevated Ag85A-specific IgG titers have been identified as a correlate of lower risk of TB disease in a post-hoc analysis of the MVA85A vaccine trial (Fletcher et al., 2016), highlighting the mounting evidence for a possible role for Abs in Mtb protective immunity.

Beyond opsonization, Abs direct innate immune antimicrobial activity via their constant (Fc) domains following engagement of FcRs found on all innate immune cells (Casadevall and Pirofski, 2006; Nimmerjahn and Ravetch, 2008). These functions, interrogated extensively in the monoclonal therapeutics field (Bakema and van Egmond, 2014), include cytolysis of infected target cells by natural killer (NK) cells and complement; clearance of target cells by monocytes, neutrophils, and dendritic cells (DCs); immune regulation in inflammation; toxin clearance and neutralization; and antigen presentation by DCs to promote adaptive immunity (Ackerman and Alter, 2013; Nimmerjahn and Ravetch, 2008). In infectious diseases, accumulating evidence points to a critical role for Fc-mediated Ab functions in influenza (DiLillo et al., 2014), HIV (Bournazos et al., 2014; Hessell et al., 2007), Ebola (Olinger et al., 2012; Schmaljohn and Lewis, 2016), and malaria (Bergmann-Leitner et al., 2006; Pleass, 2009). These Fc effector functions are regulated immunologically via two features of the Ab Fc domain: 1) through Fc class-switch recombination selecting different isotypes (i.e., IgG, IgM, IgA, IgD, and IgE) and/or subclasses (e.g., IgG1, 2, 3, 4) and 2) the post-translational addition of distinct glycan species on the Fc domain of antibodies, specifically at asparagine 297 on IgG (Vidarsson et al., 2014). In particular, Ab glycosylation varies with age, sex, disease state, treatment, infection, and vaccination which likely reflect the highly sensitive and dynamic processes that actively alter Ab effector function during an inflammatory response (Ackerman et al., 2013; Gardinassi et al., 2014; Ho et al., 2014; Mahan et al., 2016; Parekh et al., 1989).

FcRs have been implicated in immune modulation of TB disease. Mice deficient in activating FcRs exhibit enhanced immunopathology and elevated bacterial burden while those lacking the inhibitory FcR have diminished pathology (Maglione et al., 2008). Similarly, higher expression of the activating high-affinity FcγRI (Sutherland et al., 2014) and loss of the activating low-affinity FcγRIIIb are associated with enhanced TB disease (Machado et al., 2013). Thus, collectively, these lines of evidence point to a potential role for Fc-mediated Ab modulation of TB disease. Hence here we aimed to define whether distinct Ab Fc-effector functional profiles could contribute to Mtb control among individuals with latent TB (Ltb) who, though infected, successfully control Mtb such that they manifest no clinical symptoms, as compared to those with active TB disease (Atb) who lack such control. Using a systems serology approach (Chung et al., 2015), we profiled 70 Ab features associated with Fc effector activity and identified differential Ab glycosylation and functional profiles that distinguished Ltb and Atb. Moreover, Abs isolated from Ltb enhanced human macrophage control of Mtb with increased phagolysosomal fusion,

inflammasome activation, and lower bacterial burden *in vitro* compared to Atb. Together, these data highlight Ab glycosylation profiles as potential immune correlates of TB disease state and provide mechanistic insights into Ab Fc effector function in bacterial control.

Results

Ab signatures distinguish latent (Ltb) and active (Atb) TB disease

To broadly explore the humoral immune responses in TB disease, we profiled plasma derived IgG from HIV-negative individuals with Ltb (n=22) or Atb (n=20) (Table 1) from South Africa. We assessed 70 Ab features (Supplemental Table) including the ability to recruit Ab-dependent cellular phagocytosis (ADCP) and Ab-dependent cellular cytotoxicity (ADCC) (Chung et al., 2015) in response to purified protein derivative (PPD) and fractionated Mtb culture preparations; IgG Fc binding to activating (FcγRIIIa and FcγRIIa) and inhibitory (FcγRIIb) FcRs; antigen-specific IgG subclass levels; and IgG glycosylation. Principal component analysis (PCA) (Jolliffe, 1986) of the Ab features resolved divergent humoral immune profiles between the groups (Supplemental Figure 1). Feature reduction (Tibshirani, 1997) identified nine Ab characteristics as the minimal parameters that could separate the two disease states (Table 2, indicated by ^). PCA using these nine features alone segregated the Ltb individuals (blue) towards the left of the x-axis and Atb individuals (red) towards the right (Figure 1A). The mirror loadings plot (Figure 1B), where the relative location of an individual feature is associated with the geographical position of the corresponding disease state group on the dot plot (Figure 1A), highlighted differential Ab glycosylation as a feature that separated with both Ltb and Atb ($\hat{3}$, $\hat{4}$, $\hat{8}$, and $1\hat{8}$ in Figure 1B). After correction for multiple comparisons (Holm, 1979), the digalactosylated (G2) Ab glycoform was identified as the biomarker that best discriminated between the groups (Table 2, indicated by $^{\&}$). These data show that PPD-specific Fc profiles can resolve differences between Ltb and Atb Abs.

Abs generated in Ltb and Atb exhibit distinct Fc effector functional profiles

We next sought to define whether these differences in Ab Fc profiles were simply biomarkers of disease state or also contributed to immune activity against Mtb. Among the innate immune cells with potential antimicrobial function, we explored Ab activation of NK cells, monocytes, and neutrophils. On a per PPD-specific Ab level, we observed that IgG from individuals with Ltb (n=22) compared to Atb (n=20) was associated with enhanced NK cell–mediated, PPD-specific ADCC (Figure 2A, p=0.0233) and NK cell degranulation (CD107a upregulation, Figure 2B, p=0.0110). Likewise, consistent differences were observed for additional measures of NK cell activation including the secretion of MIP1β and IFN-γ (Supplemental Figure 2A-B). Ab-mediated phagocytosis of PPD-adsorbed beads trended higher in the presence of neutrophils (Figure 2C) and was significantly enhanced in Atb compared to Ltb in the presence of the monocytic cell line, THP1, (Figure 2D, p=0.0010). Similarly, enhanced monocyte-mediated phagocytosis was also observed in the presence of some but not all Mtb culture fraction–coated beads (Supplemental Figure 2C-G, p values from 0.006 to 0.011), suggesting some selectivity in Ab function against particular antigens. To further assess antigen specificity, we generated two pools of Abs composed of purified polyclonal IgG from individuals within each disease group: Ltb (n=22) and Atb

(n=20). Depletion of PPD-specific Abs resulted in trends towards reduced ADCC and ADCP and significantly reduced ADNP (Supplemental Figure 2H-J) supporting the antigen-specific nature of Ab effector activity. That bioactivity was not completely depleted may affirm immune complex biology where even low affinity Abs that remain in the pools elicit some activity. Moreover, functional differences in ADCP were not observed with uncoated control beads (Figure 2E) or beads coated with an irrelevant pool of influenza hemagglutinin proteins (Figure 2F), against which IgG titers were similar or higher to those observed for PPD (Supplemental Figure 2K), highlighting disease specific differences in Ab Fc-effector function. Together these lines of evidence suggest that distinct Ab effector profiles in Ltb and Atb can selectively recruit innate immune cell activity in an antigen specific manner.

Distinct FcR binding profiles in Ltb and Atb

Low-affinity interactions between the Ab Fc domain and activating or inhibitory FcRs regulate Fc-mediated effector functions. Low affinity FcRs include the activating FcRs, FcγRIIa and FcγRIIIa/IIIb, and the sole inhibitory FcR, FcγRIIb (Bruhns, 2012; Mishra et al., 2010). While no significant differences were observed in the capacity of Ltb and Atb IgG to bind to FcγRIIa (Figure 2G) or FcγRIIb (Figure 2H), IgG from Ltb individuals bound to the activating FcγRIIIa at significantly higher levels compared to IgG from Atb (Figure 2I, p=0.002). Sensorgram overlay for FcγRIIIa binding demonstrated that differential binding relates to enhanced on, rather than off rates, consistent with a mode of action of glyco-engineered monoclonal Abs (Supplemental Figure 2M) (Nimmerjahn and Ravetch, 2008). This difference in FcγRIIIa binding was also observed in the ratios of activating to inhibitory FcR binding (Figures 2J, p=0.0174 and K), which more accurately captures alterations in immune complex dynamics with combinations of FcRs expressed on innate immune cells (Ackerman and Alter, 2013; Pincetic et al., 2014). These results, pointing to a selectively enhanced FcγRIIIa binding profile, tracks with enhanced NK cell–mediated Fc effector function observed among Ltb Abs (Figures 2A and 2B).

Minimal differences in Mtb-specific subclass selection profiles

Ab affinity for select FcRs can be regulated via subclass selection (Chung et al., 2014b). While total Mtb-specific IgG levels trended towards higher levels in Atb (Supplemental Figure 3), no statistically significant differences were observed among the most functional Ab subclasses, IgG1 and IgG3 (Bruhns, 2012). Thus Ltb is associated with lower antigen-specific Ab titers, as would be expected in the context of a lower bacterial burden. However, subclass selection profiles alone do not account for the functional profile differences observed between the groups.

Significant differences in Ab glycosylation

A second mechanism by which the immune system naturally tunes FcR affinity is via differential glycosylation of IgG Abs at a single asparagine residue at position 297 in the CH2 domain (Arnold et al., 2007; Raju, 2008). The Fc glycan is composed of a core complex bi-antennary structure of mannose (Man) and n-acetylglucosamine (GlcNAc) with variable levels of five branching or terminal sugars: fucose (F), galactose (G), bisecting GlcNAc (B), and sialic acid (SA) (Raju, 2008). These post-translational modifications tune the affinity of Abs for FcRs and regulate effector function (Herter et al., 2014; Zou et al.,

2011). To determine whether differences in Ab glycosylation account for diverging functional profiles, glycosylation of purified IgG from individuals with Ltb and Atb were analyzed by capillary electrophoresis (CE) (Mahan et al., 2015). Unsupervised hierarchical clustering of all measured glycans (Figure 3A) showed that Ltb and Atb glycan profiles clustered as nearly distinct signatures, with a single Atb glycan profile outlier sample clustering with the Ltb samples. Despite this surprising classification accuracy between the disease groups, significant heterogeneity was observed among the glycan profiles within patient class, potentially reflecting the spectrum of latent and active disease states (Barry et al., 2009).

At a more granular level, no statistically significant difference was observed in bisecting GlcNAc (Figure 3B), the addition of which improves binding to FcγRIII (Zou et al., 2011). However, total IgG from individuals with Ltb compared to Atb contained less fucose, another modification known to enhance Ab binding to FcγRIII (Ferrara et al., 2011; Niwa et al., 2005) (Figure 3C, p=0.0041). Additionally, striking differences were observed in galactose and sialic acid levels, which are associated with inflammation (Anthony et al., 2011; Jefferis, 2009). Specifically, IgG purified from Ltb individuals had fewer “inflammatory” agalactosylated (G0) (Figure 3D, p=0.0003) and higher “anti-inflammatory” di-galactosylated (G2) structures (Figure 3E, p=0.0002). Consistent with this, IgG purified from Ltb individuals had higher levels of the “anti-inflammatory” sialic acid (S) compared to Atb (Figure 3F, p=0.0010). Parallel patterns of glycosylation were observed in PPD-specific IgG from a subset of individuals (Ltb n=6, Atb n=7) for whom sufficient sample was available (Figure 3 and Supplemental Figure 4A-E).

Given that glycan structures were many of the top potential discriminatory features in our analyses (Table 2), we sought to validate these findings in an independent, geographically distinct cohort of HIV-negative individuals with Ltb (n=10) and Atb (n=10) from Texas/Mexico (Table 1). These differences were recapitulated in this second cohort (Figure 3G-K, p values from 0.003 to 0.025) and remained significant following correction for multiple testing. To confirm the essential role of the glycan in directing Ab effector function (Olivares et al., 2013), glycans were enzymatically removed from IgG purified from a subset of age- and sex-matched pairs of individuals with Ltb (n=9) and Atb (n=9) from South Africa for whom sufficient sample was available. As expected, the removal of the glycan reduced ADCP (Supplemental Figure 4F, p<0.0001). Together, these data demonstrate that Ltb and Atb are associated with conserved differential and selective Ab glycosylation profiles that drive Ab effector function and potentially serve as biomarkers of disease state.

Distinct impacts of Abs on modulating host-mediated pathogen control

Next, we investigated whether Abs can also contribute to antimicrobial control using primary human monocyte-derived macrophages (MDM) infected with virulent Mtb (Martin et al., 2012). We focused on MDM uptake of Mtb (Figure 4A) or PPD-coated beads (Supplemental Figure 5A). Opsonization of either bacteria or beads by pools of Ltb compared to Atb IgG were not statistically significantly different.

We then sought to determine whether Abs could impact MDM control of Mtb after infection. As phagolysosomal-Mtb co-localization is a critical step in intracellular bacterial

control, we assessed the impact of Abs on this process. Mtb-infected MDM were treated with pooled IgG from Ltb or Atb individuals immediately after infection. Ltb IgG increased co-localization of Mtb with lysosomes as compared to Atb IgG (Figure 4B, p=0.0057 Ltb vs Atb), suggesting that Ltb Abs can activate antimicrobial processes within macrophages even after infection.

Recent studies have shown that Abs can activate the inflammasome in the context of malaria (Hirako et al., 2015) and autoimmune disease (Muller-Calleja et al., 2015) and that inflammasome activation may play an important role in TB infection (Briken et al., 2013). Treatment of Mtb-infected MDM with pooled Ltb as compared to Atb Abs increased the formation of perinuclear Apoptosis-associated Speck-like protein containing a Caspase Activation and Recruitment Domain (ASC) aggregates (Mishra et al., 2010), a measure of inflammasome activation (Figure 4C and D, p=0.0226 and 0.0180). In addition, IgG pooled from Ltb individuals also enhanced IL1β secretion (Figure 4E, p values from 0.001 to 0.009), a second marker of inflammasome activation (Martinon et al., 2002; McElvania Tekippe et al., 2010). Importantly, no differences in cell death were observed between MDM treated with pooled Ltb or Atb IgG (Figure 4F and Supplemental Figure 5B), reminiscent of data demonstrating that *Salmonella* activation of the NLRC4 inflammasome in neutrophils selectively promotes IL1β secretion without pyroptosis of the infected cells (Chen et al., 2014).

Next, we evaluated the effect of Ltb and Atb Abs on bacterial survival within macrophages. In a standard plating assay, treatment of MDM after Mtb infection with pooled Ltb IgG resulted in significantly lower bacterial burden compared to treatment with pooled Atb IgG (Figure 4G, p=0.0261 and 0.0047). To determine if Ltb IgG enhanced the capacity of MDM to restrict Mtb growth or truly promoted bacterial killing, an Mtb strain carrying a “live-dead” reporter was used. The “live-dead” reporter enables tracking of both cumulative bacterial burden via a long-lived constitutive fluorophore (mCherry) and the quantification of the fraction of surviving bacteria, defined by tetracycline inducible GFP expression that correlates with bacterial viability, confirmed by colony forming units (CFU) (Martin et al., 2012) (Figure 4H). Treatment of infected macrophages with Ltb Abs reduced bacterial survival compared to Atb Abs in seven of eight macrophage donors (Figure 4I, p=0.0156). While donor-to-donor variability was observed (Supplemental Figure 5C), highlighting potential nuances in innate immune cell activity, these results demonstrate that Ltb Abs promote the ability of macrophages to kill bacteria as compared to Atb Abs. Taken together, these results demonstrate that Abs isolated from individuals with Ltb have distinct glycosylation patterns linked to enhanced FcRγIIIa binding that are able to activate innate immune control of TB infection.

Discussion

While a direct role for Abs in TB has been unclear, the data presented here highlight the existence of distinct Ab Fc effector profiles that correlate with different TB disease states and suggest mechanisms by which humoral immunity may modulate pathogenesis. Using a systems serology approach, we show highly divergent Ab signatures between individuals with Ltb and Atb (Figure 1). Despite lower titers to PPD and other Mtb fractions, individuals

with Ltb possess Abs able to drive superior NK cell activation. This increased Ltb Ab functionality correlates with increased binding to the activating FcγRIII (Figure 2I-J), known to drive NK cell activation and ADCC (Ravetch and Perussia, 1989). Moreover, the divergent functional profiles observed between Ltb and Atb are associated with distinct Ab glycan profiles, validated an independent, geographically distinct cohort, highlighting the potential utility of Ab glycosylation profiles as biomarkers of disease state (Figure 3). Finally, these differences were linked to differential activation of innate immunity and Mtb killing within primary macrophages (Figure 4I), suggesting that Abs may not only mark disease states but also contribute functionally to infection outcome.

We found that beyond opsonization, Ltb Abs enhanced several macrophage responses against intracellular Mtb including phagolysosomal maturation and inflammasome activation independent of pyroptosis. The impact on inflammasome activation is particularly provocative in light of recent studies showing that circulating immune complexes containing *Plasmodium* spp. DNA (Hirako et al., 2015) or phospholipid-specific Abs can activate the inflammasome in monocytes (Muller-Calleja et al., 2015; Prinz et al., 2011). Moreover, in some TB studies, inflammasome activation has been linked to bacterial control (Carlsson et al., 2010; Eklund et al., 2014; Mishra et al., 2010; Pontillo et al., 2013). Thus, our data suggest that Abs could direct inflammasome activation in macrophages, and this may contribute to bacterial control.

How Abs recognize Mtb-infected macrophages remains unclear. Bacterial cell wall constituents have been shown to access a constitutive lysosomal exocytic pathway that fuses with the macrophage plasma membrane (Beatty et al., 2001). Thus, Abs may directly recognize antigens on the infected cell and bind to and activate FcRs in *cis* or *trans*. It is also possible that Abs may form immune complexes with soluble bacterial antigens or enter the cell through pinocytosis/endocytosis and recognize bacteria in endosomal compartments. Finally, the existence of intracellular FcRs, such as TRIM21 (McEwan et al., 2013), may allow for the recognition of bacterial components within the cytoplasm. Moreover, given that granulomas contain an array of immune cells beyond macrophages (Nunes-Alves et al., 2014; Tsai et al., 2006; Ulrichs et al., 2004), the ultimate impact of functional Abs is likely to be a product both of how they direct bacterial fate within macrophages as well as engage the collaborative activity of the local cellular microenvironment. Future studies will be required to elucidate the mechanism(s) by which Abs recognize and kill intracellular Mtb, recruit beneficial innate immune cell functions, and identify the specific Mtb targets that may be most critical for these antimicrobial activities.

The data presented here suggest that Ab Fc characteristics, including differential glycosylation, may provide a means to distinguish Ltb from Atb. In HIV infection (Ackerman et al., 2013) and autoimmune disease (Anthony et al., 2011; Jefferis, 2009; Malhotra et al., 1995; Parekh et al., 1989), antigen-specific Abs are differentially glycosylated as a function of disease state and treatment status (Ackerman et al., 2013; Gardinassi et al., 2014; Ho et al., 2014; Vidarsson et al., 2014). Moreover, recent data suggest the existence of distinct Ab glycosylation patterns between different antigen specificities (Mahan et al., 2016). Thus, Ab glycosylation differences may reflect differential B cell priming (Mahan et al., 2016; Selman et al., 2012) aimed at directing optimized

pathogen- or antigen-specific clearance activity. In autoimmune disease, Ab glycosylation is heavily influenced by inflammation (Bohm et al., 2014), and interestingly, the glycan modifications that are enriched among individuals with Atb are quite similar to those observed in rheumatoid arthritis and HIV infection (Ackerman et al., 2013; Gunn et al., 2016; Parekh et al., 1989) suggesting that high levels of agalactosylated (G0) Abs may emerge in the setting of chronic inflammatory diseases. This may be linked to the non-specific activation of B cells or the induction of unique B cell responses in the setting of persistently high antigen loads. Conversely, in controlled Ltb disease, the conversion of activated B cells to Ab-secreting cells (plasmablasts or plasma cells) may occur in a less inflammatory environment within germinal centers (GC) in lymph nodes, resulting in the induction of non-inflammatory (non-G0) but more functional Ab glycan profiles aimed at driving bacterial control. To this point, in TB disease the granuloma itself may have GC-like properties (Kahnert et al., 2007), potentially enabling unique Mtb-specific Ab profiles to be programmed within the lung even in Ltb. Where optimal B cell responses are primed and how these may be disrupted leading to bacterial escape is unclear but likely to be defined in future studies of NHPs and longitudinal cohorts that follow disease progression from Ltb to Atb.

While recent data point to the promising role of gene array technology for distinguishing Ltb and Atb (Berry et al., 2010; Zak et al., 2016), current clinical immunologic diagnostics for TB infection have been inadequate. The use of antigen-specific Ab glycan profiles would be particularly attractive clinical correlates given their ease of interrogation (Mahan et al., 2015). Importantly, because vaccination generates Ab profiles distinct from natural infection (Mahan et al., 2016; Vestrheim et al., 2014), antigen-specific Ab glycan profiles may provide diagnostic value even in an immunized population. Moreover, differences in glycosylation patterns observed in individuals with TB as compared to other chronic infections such as HIV (Supplemental Figure 6) (Mahan et al., 2016) suggest that these changes are not necessarily simply representative of a non-specific inflammatory state. Therefore, additional efforts to define the preferential antigen-specific Ab populations most sensitive to disease progression may refine our understanding of how to most effectively use Ab glycosylation states as biomarkers.

The most provocative implication of these data is that Abs may contribute to the control of TB disease. It is possible that discrepancies as to a protective or non-protective role for Abs may be resolved with appreciation for the diverse functions of Abs and how they may be regulated both by the antigens they recognize and the characteristics of their Fc domains. Because recent work suggests that it is possible to generate distinct Fc profiles through vaccination (Mahan et al., 2016), defining the features of the Abs that provide the most protection against TB infection may provide a roadmap for future vaccine design.

Methods and Resources

Contact for Reagent and Resource Sharing

Further information and requests for reagents may be directed to and will be fulfilled by the corresponding author and lead contact Galit Alter (galter@mgh.harvard.edu).

Experimental Model and Subject Details

Study population and sample collection

Twenty-two adult HIV-seronegative individuals with Ltb and twenty with Atb were recruited from Cape Town, South Africa (Day et al., 2011) (Table 1). Ltb was defined by the presence of IFN-γ-producing T cells specific for CFP10 and ESAT6 in whole blood intracellular cytokine staining (ICS), with no previous history of TB diagnosis, treatment or active clinical symptoms. Atb was defined by positive sputum smear microscopy or culture for *M. tuberculosis* (Mtb). Peripheral blood was obtained in sodium heparin Vacutainer tubes (BD Biosciences) and plasma isolated by Ficoll-Histopaque (Sigma-Aldrich) density centrifugation within 4 hr of collection. Blood was obtained from Ltb individuals in the absence of therapy and from Atb individuals between 0 and 7 days after initiation of therapy per South African National Health Guidelines. All study participants gave written, informed consent, approved by the Human Research Ethics Committee of the University of Cape Town and the Western Cape Department of Health.

Ten adult HIV seronegative individuals with Ltb and ten with Atb were recruited from the south Texas (USA)/north-eastern Mexico regions (Restrepo et al., 2011) (Table 1). Ltb was defined by the presence of positive tuberculin skin test and/or IFN-γ-producing T cells specific for CFP10 and/or ESAT6 peptides with no previous history of TB diagnosis, treatment or active clinical symptoms. Atb was defined by either positive sputum smear microscopy, positive culture for Mtb and/or clinical diagnosis when microbiological test results were negative or unavailable (clinical case: symptoms compatible with Atb and documentation of TB treatment for at least 6 months). All study participants gave written, informed consent, approved by the institutional review boards of the participating institutions in Mexico and the United States.

Healthy HIV-seronegative donors in the Boston, Massachusetts (USA) area were recruited by Ragon Institute of MGH, MIT, and Harvard, whole blood collected in ACD tubes and plasma was isolated as detailed above. All study participants gave written, informed consent, approved by the institutional review boards at Massachusetts General Hospital and Partners Healthcare.

Primary Monocyte Derived Macrophages

CD14-positive cells were isolated from whole blood from seronegative donors using the EasySep CD14 Selection Kit per the manufacturer's instructions (Stem Cell Technologies) and matured for 7 days in RPMI (Invitrogen) with 10% fetal calf serum (Life Technologies) in low-adherent flasks (Corning). Monocyte-derived macrophages (MDM; 5×10^4 per well) were plated in a glass bottom 96-well plates (Greiner) 24 hr prior to Mtb infection or addition of Ab-opsonized, PPD-adsorbed beads or Mtb.

M. tuberculosis H37Rv

Live dead reporter bacteria constitutively express mCherry and a tetracycline inducible GFP (Martin et al., 2012). Bacteria were cultured in 0.5 mg/ml Hygromycin 7H9 media (BD) at 37°C in log phase, washed, sonicated and passed through 5 μm filter (Millex) to obtain a

single cell suspension prior to infection at multiplicity of infection (MOI) 1 for 14 hrs at 37°C. For experiments involving induction of GFP fluorescence expression in transcriptionally active bacteria, anhydrotetracycline (Sigma) (200 ng/mL) was added for 16 hours.

Method Details

Antigens

Mtb antigens used were: PPD (Statens Serum Institute), cell membrane, culture filtrate, cytosol protein, soluble cell wall protein and soluble protein fractions of H37RV Mtb (BEI Resources). A mixture of seven recombinant influenza envelope HA antigens representative of the dominant strains in the past 10 years were used as a control: H1N1-A/Brisbane/59/2007, B/Florida/4/2006), B/Malaysia/2506/2004, H1N1-A/Solomon Island/3/2006, H3N2-A/Wisconsin/67/X-161/2005, H3N2-A/Brisbane/10/2007), H1N1-A/New Caledonia/20/99 (all from Immune Technology Corp.).

Isolation of bulk IgG

Total IgG was purified from plasma via negative selection using Melon Gel resin (Thermo Scientific). All purified IgGs, except endotoxin contaminated monoclonal Abs used as controls for endotoxin removal, were filtered through 0.2 μM (Fisher) and 300 kDa filters (Amicon) prior to use. Endotoxin levels were assayed by LAL Chromogenic Endotoxin Quantitation Kit (Pierce). No effect of endotoxin was observed in the purified Abs or pools in functional assays (Supplemental Figure 2L and 5D).

Isolation of PPD-specific IgG

Purified protein derivative (PPD) was biotinylated with Sulfo-NHS-LC-LC Biotin (Thermo Scientific) and coated onto M270 Streptavidin Dynabeads (Invitrogen). Subject plasma was incubated with PPD-conjugated beads at 4°C for 24 hrs. Beads were washed with PBS (Corning), and PPD-specific IgG was eluted using 100mM citric acid (pH 3.0) and neutralized with 0.5 M potassium phosphate (pH 9.0).

IgG pools

Pools of Ltb and Atb Ab were generated by mixing equivalent total IgG from each individual Ltb (n=22) or Atb (n=20) sample. The resulting pools were passed through a 300 kDa centrifugal filter (Amicon) to remove immunoglobulin complexes. Human IgG from over 1000 healthy North American donors (Sigma) was used as a control and also passed through a 300 kDa filter.

PPD-specific IgG depletion

Biotinylated PPD was coated on 1 mm fluorescent neutravidin beads (ThermoFisher) and incubated with Ab pool mixes at 4°C for 16 hrs. PPD-specific IgG was pulled down, and the depleted pools removed for further use. Depletion was confirmed by PPD ELISA (data not shown).

IgG deglycosylation

To remove N-linked glycans from IgG, 100 μg of purified IgG (0.8 mg/mL) was treated with 6250 U PNGase enzyme (NEB) or control water at 37°C for 14 hrs in 50 mM sodium phosphate. The reactions were passed through 50 kDa centrifugal filters (Amicon) to remove the enzyme and then used for functional assays.

IgG quantitation

Total IgG concentrations were determined by Human IgG ELISA kit (Mabtech). Each sample was run in duplicate.

PPD- and HA-specific IgG quantitation

To determine PPD-specific and HA- specific IgG titers, ELISA plates (Nunc) were coated with PPD (250 ng/ml), HA-Flu (250 ng/mL), or PBS-5% BSA at 4°C for 16 hrs. The coated plates were blocked with PBS-5% BSA for 2 hrs at room temperature (RT). IgG samples were added, and the plates were incubated at RT for 2 hrs. HRP-conjugated anti-human IgG (1:500 in PBS; R&D Systems) was added, and the plates were incubated for1 hr at RT. Wells were developed in 0.4 mg/ml o-phenylenediamine in PBS/H_2O_2 and stopped by the addition of 2.5 M H_2SO_4. Absorbances were measured at 492 and 605 nm.

THP1 phagocytosis assay

The THP1 phagocytosis assay of antigen-coated beads was conducted as previously described (Ackerman et al., 2011). Briefly, Mtb antigens were biotinylated with Sulfo-NHS-LC Biotin (Thermofisher). A mixture of seven recombinant influenza HA antigens representative of the dominant strains in the past 10 years were used as a control. Biotinylated Mtb and HA antigens were incubated with 1 μm fluorescent neutravidin beads (Invitrogen) at 4°C for 16 hrs. Excess antigen was washed away. Antigen coated beads were incubated with IgG samples (100 μg/ml) 2 hrs at 37°C. THP1 cells (1×10^5 per well) were added and incubated at 37°C for 16 hrs. Bead uptake was measured in fixed cells using flow cytometry on a BD LSRII equipped with high-throughput sampler. Phagocytic scores are presented as the integrated MFI (% bead-positive frequency × MFI/10,000) (Darrah et al., 2007) (Supplemental Figure 7). ADCP experiments for individual IgG samples were performed in duplicate in three independent experiments, while pooled IgG samples were tested in duplicate in two independent experiments.

ADCC assay—A modified rapid fluorometric ADCC (RFADCC) assay was used (Chung et al., 2014b; Gomez-Roman et al., 2006). CEM-NKr CCR5+ cells (NIH AIDS reagents) were pulsed with PPD (60 μg/ml) for 1 hr at RT and labeled with the intracellular dye CFSE (Sigma) and the membrane dye PKH26 (Invitrogen). NK cells were isolated from seronegative donor whole blood with RosetteSep (Stem Cell Technologies). Purified IgG (100 μg/ml) was added to the labeled CEM-NKr cells (2×10^4 per well), incubated with NK cells (2×10^5 cells per well) for 4 hr at 37°C and fixed. The proportion of PKH26+ cells lacking intracellular CFSE staining (i.e., percent dead cells) was determined using flow cytometry (Supplemental Figure 7). Individual IgG samples were tested in two independent

RFADCC experiments, while pooled IgG samples were tested in duplicate in two experiments.

Ab-dependent NK cell activation

An ELISA-based Ab-dependent NK cell activation assays were modified for use with Mtb antigens (Jegaskanda et al., 2013). Briefly, ELISA plates (Thermo Fisher NUNC MaxiSorp flat bottom) were coated with PPD (300 ng/well) or BSA as a negative control at 4°C for 16 hrs. Purified IgG (25 μg) was added to each well. NK cells were isolated from whole blood from seronegative donors with RosetteSep (Stem Cell Technologies). NK cells (5×10^4 per well), anti-CD107a-phycoerythrin (PE)-Cy5 (BD), brefeldin A (10 mg/ml) (Sigma), and GolgiStop (BD) were added to each well, and the plates were incubated for 5 hrs at 37°C. Cells were then stained for surface markers using anti-CD16–allophycocyanin (APC)-Cy7 (BD), anti-CD56-PE-Cy7 (BD), and anti-CD3-AlexaFluor 700 (BD), and then stained intracellularly with anti-IFNγ-APC (BD) and anti-MIP1β-PE (BD) using Fix and Perm A and B solutions (ThermoFisher). Fixed cells were analyzed by flow cytometry. NK cells were defined as CD3- and CD16/56+. Ab-dependent NK cell activation assays were performed in two independent experiments.

Ab-dependent Neutrophil activation

Whole healthy donor blood was mixed with an equal volume of 3% dextran-500 (ThermoFisher) and incubated for 25 min at RT to pellet the red blood cells. Leukocytes were removed and washed in HBSS without calcium and magnesium (ThermoFisher). The leukocytes were further separated using Ficoll-Histopaque (Sigma-Aldrich) centrifugation, and the granulocyte pellet was harvested and washed with PBS. PPD conjugated beads, as described above, were incubated with IgG (100 μg/mL) for 2 hrs at 37°C. Isolated neutrophils (1×10^5 per well) were added and incubated for 16 hrs at 37°C. Bead uptake was measured by flow cytometry as described above. The purity of neutrophils was confirmed by staining with CD66b (BioLegend). Pooled IgG samples were tested in duplicate in three independent experiments

FcγR Surface Plasmon Resonance Analysis

Surface plasmon resonance (SPR) assays were performed on a Biacore 3000 (Chung et al., 2014a). Research grade CM5 plasmon surface resonance chips (GE) were coated with recombinant FcγRIIa, IIb, IIIa (R&D Systems), or PBS control. Purified IgG (100 μg/ml) was used to assess the binding of Abs to the individual FcγRs based on the area under the curve quantified by the relative response units (RU) of signal following injection. Individual IgG samples were tested twice. After each assay cycle, the sensor chip surface was regenerated using 10 mM glycine pH 3.0. Binding response was recorded as RU continuously, with background binding automatically subtracted.

Antigen-specific IgG subclass quantitation

A customized Luminex subclass assay (Brown et al., 2012) was used to quantify the relative concentration of each Ab isotype among Mtb antigen-specific Abs. Carboxylated microspheres (Luminex) were coupled with Mtb protein antigens by covalent NHS-ester

linkages via EDC and NHS (Thermo Scientific) per the manufacturer's instructions. Antigen-coated microspheres (5000 per well) were added to a 96-well filter plate (Millipore). Each IgG sample (5 μg of bulk IgG) was added to five replicate wells of a 96-well plate and incubated 16 hrs at 4°C. The microspheres were washed, and IgG1-, IgG2-, IgG3-, IgG4-, or bulk IgG-specific detection reagents (Southern Biotech) were added for 2 hr at RT. The beads were then washed and read on a Bio-Plex 200 System. The background signal, defined as MFI of microspheres incubated with PBS, was subtracted. Each sample was tested twice.

Glycan profiling of IgG

Purified bulk (10 μg) or PPD-specific IgG was denatured and treated with PNGase enzyme (NEB) to release N-linked glycans (Mahan et al., 2015). Proteins were precipitated in ice-cold ethanol, and the glycan-containing supernatants were dried using a CentriVap. The dried glycans were fluorescently labeled with a 1:1 ratio of 50 mM APTS (8-aminoinopyrene-1,3,6-trisulfonic acid, ThermoFisher) in 1.2 M citric acid and 1 M sodium cyanoborohydride in tetrahydrofuran (Sigma-Aldrich) at 55°C for 2 hr. The labeled glycans were dissolved in water, and excess unbound APTS was removed using Bio-Gel P-2 (Bio-rad) size exclusion resin. Samples were run with a LIZ 600 DNA ladder in Hi-Di formamide (ThermoFisher) on an ABI 3130XLl DNA sequencer. Data were analyzed using GeneMapper (Chatterji and Pachter, 2006) software, and peaks were assigned based on migration of known standards and glycan digests. Peak area was calculated, and the relative percentage of each glycan structure is graphed.

In vitro macrophage opsonophagocytosis

For Mtb and PPD-adsorbed bead uptake experiments, pooled IgG (100 μg/mL) and Mtb or PPD-adsorbed fluorescent beads described above were incubated 37°C for 1 hr prior to infection at an MOI of 1 for 4–6 hrs at 37°C. The cells were washed, fixed, and stained with DAPI (Sigma; 500 ng/mL) in 0.1% IGEPAL CA-630 (Sigma) for 10 min at RT. Images were obtained using an Operetta High-Content Imaging Fluorescence Microscope (Perkin-Elmer) with 20× NA objective. Mtb in macrophages was quantified based on Alexa-546+ pixels. Fluorescent PPD-adsorbed beads in macrophages were quantified based on Alexa-488+ pixels. Bacterial or PPD-bead uptake per macrophage as determined by DAPI was scored. The ratio of bacterial uptake in the presence of Ltb or Atb to bacterial uptake in the absence of an Ab was used to calculate the relative Mtb uptake (Ltb or Atb/No IgG). Between 1.5×10^4 and 4×10^4 cells per condition over technical triplicates per donor were analyzed via CellProfiler (Carpenter et al., 2006; Martin et al., 2012). Mtb uptake was tested in triplicate in three healthy macrophage donors. Fluorescent PPD-adsorbed bead uptake was tested in triplicate in two healthy macrophage donors.

Mtb-phagolysosomal co-localization

For co-localization of Mtb in lysosomes, pooled IgG (100 μg/ml) samples were added to MDM infected with mCherry-expressing Mtb as described above for 96 hrs at 37°C. Lysotracker Deep Red (1 mM; ThermoFisher) was added to samples for 1 hr at 37°C prior to washing and fixation. Macrophage nuclei stained with DAPI (Sigma; 500 ng/mL) in 0.1% IGEPAL CA-630 (Sigma) for 10 min at RT, and the cells were washed. . Images were

obtained using a Zeiss LSM 510 Confocal Microscope fitted with a 20× objective. Between 200 and 600 macrophages per condition over technical duplicates per donor (total two) were analyzed using CellProfiler (Martin et al., 2012). Single-cell data was extrapolated using a custom Python script and plotted as violin plots that show the distribution of co-localization rates (or "percent co-localization") represented by kernel density estimations in macrophages under each condition. Each condition was tested in duplicate in two healthy macrophage donors.

Inflammasome activation in macrophages

Pooled IgG (100 μg/ml) samples were added to MDM infected with mCherry-expressing Mtb as described above for 96 hrs at 37°C. Culture supernatants were collected for analysis of IL1β levels by ELISA as described below. Cells were washed, fixed, and stained with DAPI. For ASC staining, after fixation, the samples were blocked in 0.1% saponin/0.2% BSA for 30 min at RT, washed, and incubated with anti-ASC (Adipogen; 1:200) for 1 hr at RT. The samples were washed again and stained with a AlexaFluor 647–conjugated goat anti-rabbit secondary antibody (ThermoFisher; 1:500) for 1 hr at RT. Images were obtained using a Zeiss LSM 510 Confocal Microscope fitted with a 20× objective. Between 200 and 600 cells per condition over technical duplicates per donor (total two) were analyzed by ImageJ. ASC puncta per nuclei as determined by DAPI was scored. ASC puncta per nuclei in the presence of Ltb or Atb to control Sigma IgG (sIgG) was used to calculate the relative ASC speck per macrophage (Ltb or Atb/control sIgG). For ASC staining, each condition was tested in duplicate in two healthy macrophage donors. Human IL1β levels in the culture supernatants were determined using a Human IL1β Ultrasensitive ELISA kit (Novex Life Technologies). The level of IL1β in the presence of Ltb or Atb to the absence of Ab was used to calculate the relative IL1β level (Ltb or Atb/no IgG). Each condition was tested in triplicate in four healthy macrophage donors.

TUNEL assay

Pooled IgG (100 μg/ml) samples were added to MDM infected with mCherry-expressing Mtb as described above for 96 hrs at 37°C. TUNEL (Promega) staining was performed per manufacturer instructions. Images were obtained via Zeiss LSM 510 Confocal Microscope outfitted with a 20× objective. Between 200 and 600 cells per condition over technical duplicates per donor (total two) were analyzed using CellProfiler (Carpenter et al., 2006; Martin et al., 2012). Apoptosis was scored as cells possessing a TUNEL+ pyknotic nucleus. Each condition was tested in duplicate in two healthy macrophage donors.

in vitro macrophage Mtb survival

Pooled IgG (100 μg/ml) samples were added to MDM infected with mCherry-expressing Mtb as described above for 96 hrs at 37°C. Eighty hours post infection, 200 ng/mL anhydrotetracycline (Sigma) was added for the next 16 hours to induce GFP expression in live but not dead bacteria. The cells were washed, fixed, and stained with DAPI. Images were obtained via Operetta High-Content Imaging Fluorescence Microscope (Perkin-Elmer) outfitted with 20× NA objective. Total Mtb bacterial burden was determined based on mCherry+ pixels. Transcriptionally active Mtb bacterial burden was determined based on GFP+ pixels. Between 1.5×10^4 and 4×10^4 cells per condition over technical duplicates per

donor were analyzed using CellProfiler (Carpenter et al., 2006; Martin et al., 2012). Bacterial survival was calculated as a ratio of live to total bacteria (the number of GFP+ pixels (live) divided by the number of mCherry+ pixels (total burden). The ratio of bacterial survival in the presence of Ltb or Atb to the absence of an Ab was used to calculate the relative Mtb survival (Ltb or $Atb_{live/total}$/No $IgG_{live/total}$). The relative difference in bacterial survival was calculated as ($Ltb_{live/total}$ -$Atb_{live/total}$)/$Atb_{live/total}$. Each condition was tested in duplicate or triplicate in eight healthy macrophage donors.

For endotoxin experiments, control IgG (100 μg/mL) (Sigma) and LPS (Sigma) at increasing concentrations were added (0, 0.5 pg/mL, 1 pg/mL, 2.5 pg/mL, 5 pg/mL, 10 pg/ml, 100 pg/mL, 1 ng/mL, 10 ng/mL, 100 ng/mL and 1 μg/mL) and co-cultured with Mtb infected cells for 96 hrs at 37°C. Cells were washed, fixed, and stained with DAPI (. Images were obtained using an Operetta High-Content Imaging Fluorescence Microscope (Perkin-Elmer) outfitted with 20× NA objective. Total Mtb bacterial burden was determined based on mCherry+ pixels, and the data is reported as the pixel area per macrophage as determined by DAPI. Between 1.5×10^4 and 4×10^4 cells per condition over technical triplicates per donor were analyzed using CellProfiler (Carpenter et al., 2006; Martin et al., 2012). Each condition was tested in triplicate in three healthy macrophage donors.

Colony forming units

Pooled IgG (100 μg/ml) samples were added to MDM infected with mCherry-expressing Mtb as described above for 96 hrs at 37°C. Supernatants were collected, and the cells were washed and lysed in 80 μL of 1% Triton-X for 10 minutes at RT. Experimental conditions were performed in duplicate. Each duplicate was serially diluted tenfold and 100 μL of the 1:100, 1:1000 and 1:10,000 dilutions were plated on 7H10 (BD) plates in triplicate and incubated at 37°C for 21 days before counting. This experiment was performed using two healthy macrophage donors.

Quantification and Statistical Analysis

Statistical analysis and graphing were performed using GraphPad Prism 5.0, JMP Pro12, R, and Matlab. Data are summarized using descriptive measures such as mean, standard error, median, inter quartile range (IQR), frequency, and percent (%). Spearman's rank correlations were used to examine bivariate associations between variables. Mann-Whitney U tests were used to compare the study variables between individuals with Ltb and Atb infection (Figure 2, Figure 3B-K, Supplemental Figure 2A-G, K, Supplemental Figure 3, Supplemental Figure 4A-E) and Mtb/lysosomal co-localization of a population of macrophages treated with Ltb Abs and another with Atb Abs (Figure 4B). Kruskal-Wallis H tests with Dunn's multiple comparisons test were used to compare Ab pools with and without PPD-specific IgG fractions (Supplemental Figure 2H-J and Supplemental Figure 5A). Wilcoxon matched pair signed rank tests were used to compare Ltb and Atb matched to the same donor to the *in vitro* macrophage assays (Figure 4A, F and I) and treatment before or after PNGase (Supplemental Figure 4F). Two sample t tests were used for single comparisons of the impact of pools of Ltb or Atb Abs in assays with technical replicates in Figure 4D, E, and G and Supplemental Figure 5B. Multiple robust regression models were used to adjust for the

effect of age and sex when comparing the study variables between the two groups of individuals. Hierarchical cluster analysis using Pearson correlation was used to identify study subjects with similar features or outcome variables (Figure 3A). Principal component analysis (Jolliffe, 1986) and penalized regression using the least absolute shrinkage and selection operator (LASSO) (Tibshirani, 1997) method were used to reduce the dimension of the outcome variables (Figure 1 and Supplemental Figure 1). Cross-validation was used to find the optimal value of the regularization parameter. Sixty-nine of the seventy total Ab features were used in analysis as only these features had data available on a per individual basis for these analyses. All p values are two-sided, and $p < 0.05$ was considered significant. Where appropriate, correction for multiple comparisons was performed by using the Holm-Bonferroni method (Holm, 1979). In figures, asterisks denote statistical significance (* $p \leq 0.05$; ** $p \leq 0.01$; *** $p \leq 0.001$; ns= not significant) with comparisons specified by connecting lines.

Supplementary Material

Refer to Web version on PubMed Central for supplementary material.

Acknowledgments

CEM.NKR-CCR5 was obtained through the AIDS Research and Reference Reagent Program, Division of AIDS, NIAID, NIH. The following reagents were obtained through BEI Resources, NIAID, NIH: cell membrane, culture filtrate, cytosol protein, soluble cell wall protein and soluble protein fractions of H37RV *M. tuberculosis*. We thank Peter Sorger for access to Operetta High-Content Imaging Fluorescence Microscope; Rebecca Gelman, Director of the Harvard Center for AIDS Biostatistics Core, for her advice; and many additional members of the SATVI team who helped with enrollment and evaluation of participants. This work was supported by: NIH with grants R01 AI080289 and AI102660 (GA), Dr. Dan Wattendorf and DARPA BAA-11-65 (GA), Harvard University Center for AIDS Research (CFAR) P30 AI060354 (GA, SMF, TR, MG, Ragon BL3 and Imaging Core Facility), T32 AI007387 (LL), NHMRC APP1036470 (AWC), Bill and Melinda Gates Foundation CAVD (OPP1032817: Leveraging Antibody Effector Function) (GA), Pozen Family Foundation (SMF), Doris Duke Medical Research Foundation (SMF), Burroughs Wellcome Foundation (SMF) and Ragon Institute of MGH, MIT and Harvard.

References

Achkar JM, Chan J, Casadevall A. B cells and antibodies in the defense against Mycobacterium tuberculosis infection. Immunol Rev. 2015; 264:167–181. [PubMed: 25703559]

Ackerman ME, Alter G. Opportunities to exploit non-neutralizing HIV-specific antibody activity. Current HIV research. 2013; 11:365–377. [PubMed: 24191934]

Ackerman ME, Crispin M, Yu X, Baruah K, Boesch AW, Harvey DJ, Dugast AS, Heizen EL, Ercan A, Choi I, et al. Natural variation in Fc glycosylation of HIV-specific antibodies impacts antiviral activity. J Clin Invest. 2013; 123:2183–2192. [PubMed: 23563315]

Ackerman ME, Moldt B, Wyatt RT, Dugast AS, McAndrew E, Tsoukas S, Jost S, Berger CT, Sciaranghella G, Liu Q, et al. A robust, high-throughput assay to determine the phagocytic activity of clinical antibody samples. Journal of immunological methods. 2011; 366:8–19. [PubMed: 21192942]

Anthony RM, Kobayashi T, Wermeling F, Ravetch JV. Intravenous gammaglobulin suppresses inflammation through a novel T(H)2 pathway. Nature. 2011; 475:110–113. [PubMed: 21685887]

Arnold JN, Wormald MR, Sim RB, Rudd PM, Dwek RA. The impact of glycosylation on the biological function and structure of human immunoglobulins. Annual review of immunology. 2007; 25:21–50.

Bakema JE, van Egmond M. Fc receptor-dependent mechanisms of monoclonal antibody therapy of cancer. Curr Top Microbiol Immunol. 2014; 382:373–392. [PubMed: 25116109]

Balu S, Reljic R, Lewis MJ, Pleass RJ, McIntosh R, van Kooten C, van Egmond M, Challacombe S, Woof JM, Ivanyi J. A novel human IgA monoclonal antibody protects against tuberculosis. Journal of immunology. 2011; 186:3113–3119.

Barry CE 3rd, Boshoff HI, Dartois V, Dick T, Ehrt S, Flynn J, Schnappinger D, Wilkinson RJ, Young D. The spectrum of latent tuberculosis: rethinking the biology and intervention strategies. Nat Rev Microbiol. 2009; 7:845–855. [PubMed: 19855401]

Beatty WL, Ullrich HJ, Russell DG. Mycobacterial surface moieties are released from infected macrophages by a constitutive exocytic event. Eur J Cell Biol. 2001; 80:31–40. [PubMed: 11211933]

Bergmann-Leitner ES, Duncan EH, Mullen GE, Burge JR, Khan F, Long CA, Angov E, Lyon JA. Critical evaluation of different methods for measuring the functional activity of antibodies against malaria blood stage antigens. Am J Trop Med Hyg. 2006; 75:437–442. [PubMed: 16968918]

Berry MP, Graham CM, McNab FW, Xu Z, Bloch SA, Oni T, Wilkinson KA, Banchereau R, Skinner J, Wilkinson RJ, et al. An interferon-inducible neutrophil-driven blood transcriptional signature in human tuberculosis. Nature. 2010; 466:973–977. [PubMed: 20725040]

Bohm S, Kao D, Nimmerjahn F. Sweet and sour: the role of glycosylation for the anti-inflammatory activity of immunoglobulin G. Curr Top Microbiol Immunol. 2014; 382:393–417. [PubMed: 25116110]

Bournazos S, Klein F, Pietzsch J, Seaman MS, Nussenzweig MC, Ravetch JV. Broadly Neutralizing Anti-HIV-1 Antibodies Require Fc Effector Functions for In Vivo Activity. Cell. 2014; 158:1243–1253. [PubMed: 25215485]

Briken V, Ahlbrand SE, Shah S. Mycobacterium tuberculosis and the host cell inflammasome: a complex relationship. Front Cell Infect Microbiol. 2013; 3:62. [PubMed: 24130966]

Brown EP, Licht AF, Dugast AS, Choi I, Bailey-Kellogg C, Alter G, Ackerman ME. High-throughput, multiplexed IgG subclassing of antigen-specific antibodies from clinical samples. Journal of immunological methods. 2012; 386:117–123. [PubMed: 23023091]

Bruhns P. Properties of mouse and human IgG receptors and their contribution to disease models. Blood. 2012; 119:5640–5649. [PubMed: 22535666]

Carlsson F, Kim J, Dumitru C, Barck KH, Carano RA, Sun M, Diehl L, Brown EJ. Host-detrimental role of Esx-1-mediated inflammasome activation in mycobacterial infection. PLoS pathogens. 2010; 6:e1000895. [PubMed: 20463815]

Carpenter AE, Jones TR, Lamprecht MR, Clarke C, Kang IH, Friman O, Guertin DA, Chang JH, Lindquist RA, Moffat J, et al. CellProfiler: image analysis software for identifying and quantifying cell phenotypes. Genome Biol. 2006; 7:R100. [PubMed: 17076895]

Casadevall A, Pirofski LA. A reappraisal of humoral immunity based on mechanisms of antibody-mediated protection against intracellular pathogens. Adv Immunol. 2006; 91:1–44. [PubMed: 16938537]

Chatterji S, Pachter L. Reference based annotation with GeneMapper. Genome Biol. 2006; 7:R29. [PubMed: 16600017]

Chen KW, Gross CJ, Sotomayor FV, Stacey KJ, Tschopp J, Sweet MJ, Schroder K. The neutrophil NLRC4 inflammasome selectively promotes IL-1beta maturation without pyroptosis during acute Salmonella challenge. Cell Rep. 2014; 8:570–582. [PubMed: 25043180]

Chen T, Blanc C, Eder AZ, Prados-Rosales R, Souza ACO, Kim RS, Glatman-Freedman A, Joe M, Bai Y, Lowary TL, et al. Association of Human Antibodies to Arabinomannan with Enhanced Mycobacterial Opsonophagocytosis and Intracellular Growth Reduction. Journal of Infectious Diseases. 2016

Chung AW, Crispin M, Pritchard L, Robinson H, Gorny MK, Yu X, Bailey-Kellogg C, Ackerman ME, Scanlan C, Zolla-Pazner S, et al. Identification of antibody glycosylation structures that predict monoclonal antibody Fc-effector function. AIDS. 2014a; 28:2523–2530. [PubMed: 25160934]

Chung AW, Ghebremichael M, Robinson H, Brown E, Choi I, Lane S, Dugast AS, Schoen MK, Rolland M, Suscovich TJ, et al. Polyfunctional Fc-effector profiles mediated by IgG subclass selection distinguish RV144 and VAX003 vaccines. Science translational medicine. 2014b; 6:228ra238.

Chung AW, Kumar MP, Arnold KB, Yu WH, Schoen MK, Dunphy LJ, Suscovich TJ, Frahm N, Linde C, Mahan AE, et al. Dissecting Polyclonal Vaccine-Induced Humoral Immunity against HIV Using Systems Serology. Cell. 2015; 163:988–998. [PubMed: 26544943]

Darrah PA, Patel DT, De Luca PM, Lindsay RW, Davey DF, Flynn BJ, Hoff ST, Andersen P, Reed SG, Morris SL, et al. Multifunctional TH1 cells define a correlate of vaccine-mediated protection against Leishmania major. Nat Med. 2007; 13:843–850. [PubMed: 17558415]

Day CL, Abrahams DA, Lerumo L, Janse van Rensburg E, Stone L, O'Rie T, Pienaar B, de Kock M, Kaplan G, Mahomed H, et al. Functional capacity of Mycobacterium tuberculosis-specific T cell responses in humans is associated with mycobacterial load. Journal of immunology. 2011; 187:2222–2232.

de Valliere S, Abate G, Blazevic A, Heuertz RM, Hoft DF. Enhancement of innate and cell-mediated immunity by antimycobacterial antibodies. Infect Immun. 2005; 73:6711–6720. [PubMed: 16177348]

DiLillo DJ, Tan GS, Palese P, Ravetch JV. Broadly neutralizing hemagglutinin stalk-specific antibodies require FcgammaR interactions for protection against influenza virus in vivo. Nat Med. 2014; 20:143–151. [PubMed: 24412922]

Doherty M, Wallis RS, Zumla A. group, W.H.-T.D.R.E.C.j.e.c. Biomarkers for tuberculosis disease status and diagnosis. Curr Opin Pulm Med. 2009; 15:181–187. [PubMed: 19396972]

Eklund D, Welin A, Andersson H, Verma D, Soderkvist P, Stendahl O, Sarndahl E, Lerm M. Human gene variants linked to enhanced NLRP3 activity limit intramacrophage growth of Mycobacterium tuberculosis. The Journal of infectious diseases. 2014; 209:749–753. [PubMed: 24158955]

Ferrara C, Grau S, Jager C, Sondermann P, Brunker P, Waldhauer I, Hennig M, Ruf A, Rufer AC, Stihle M, et al. Unique carbohydrate-carbohydrate interactions are required for high affinity binding between FcgammaRIII and antibodies lacking core fucose. Proceedings of the National Academy of Sciences of the United States of America. 2011; 108:12669–12674. [PubMed: 21768335]

Fletcher HA, Snowden MA, Landry B, Rida W, Satti I, Harris SA, Matsumiya M, Tanner R, O'Shea MK, Dheenadhayalan V, et al. T-cell activation is an immune correlate of risk in BCG vaccinated infants. Nat Commun. 2016; 7

Gardinassi LG, Dotz V, Hipgrave Ederveen A, de Almeida RP, Nery Costa CH, Costa DL, de Jesus AR, Mayboroda OA, Garcia GR, Wuhrer M, et al. Clinical severity of visceral leishmaniasis is associated with changes in immunoglobulin g fc N-glycosylation. MBio. 2014; 5:e01844. [PubMed: 25467439]

Glatman-Freedman A, Casadevall A. Serum therapy for tuberculosis revisited: reappraisal of the role of antibody-mediated immunity against Mycobacterium tuberculosis. Clinical microbiology reviews. 1998; 11:514–532. [PubMed: 9665981]

Gomez-Roman VR, Florese RH, Patterson LJ, Peng B, Venzon D, Aldrich K, Robert-Guroff M. A simplified method for the rapid fluorometric assessment of antibody-dependent cell-mediated cytotoxicity. Journal of immunological methods. 2006; 308:53–67. [PubMed: 16343526]

Gunn BM, Schneider JR, Shansab M, Bastian AR, Fahrbach KM, Smith ADt, Mahan AE, Karim MM, Licht AF, Zvonar I, et al. Enhanced binding of antibodies generated during chronic HIV infection to mucus component MUC16. Mucosal Immunol. 2016

Hamasur B, Haile M, Pawlowski A, Schroder U, Kallenius G, Svenson SB. A mycobacterial lipoarabinomannan specific monoclonal antibody and its F(ab') fragment prolong survival of mice infected with Mycobacterium tuberculosis. Clinical and experimental immunology. 2004; 138:30–38. [PubMed: 15373902]

Herter S, Birk MC, Klein C, Gerdes C, Umana P, Bacac M. Glycoengineering of therapeutic antibodies enhances monocyte/macrophage-mediated phagocytosis and cytotoxicity. Journal of immunology. 2014; 192:2252–2260.

Hessell AJ, Hangartner L, Hunter M, Havenith CE, Beurskens FJ, Bakker JM, Lanigan CM, Landucci G, Forthal DN, Parren PW, et al. Fc receptor but not complement binding is important in antibody protection against HIV. Nature. 2007; 449:101–104. [PubMed: 17805298]

Hirako IC, Gallego-Marin C, Ataide MA, Andrade WA, Gravina H, Rocha BC, de Oliveira RB, Pereira DB, Vinetz J, Diamond B, et al. DNA-Containing Immunocomplexes Promote Inflammasome

Assembly and Release of Pyrogenic Cytokines by CD14+ CD16+ CD64high CD32. low Inflammatory Monocytes from Malaria Patients MBio. 2015; 6

Ho CH, Chien RN, Cheng PN, Liu CK, Su CS, Wu IC, Liu WC, Chen SH, Chang TT. Association of serum IgG N-glycome and transforming growth factor-beta1 with hepatitis B virus e antigen seroconversion during entecavir therapy. Antiviral Res. 2014; 111:121–128. [PubMed: 25260899]

Holm S. A simple sequentially rejective multiple test procedure. Scandinavian Journal of Statistics. 1979; 6:65–70.

Jefferis R. Glycosylation as a strategy to improve antibody-based therapeutics. Nature reviews Drug discovery. 2009; 8:226–234. [PubMed: 19247305]

Jegaskanda S, Weinfurter JT, Friedrich TC, Kent SJ. Antibody-dependent cellular cytotoxicity is associated with control of pandemic H1N1 influenza virus infection of macaques. J Virol. 2013; 87:5512–5522. [PubMed: 23468501]

Jolliffe, I. Principal Component Analysis. Vol. 195. New York: Spinrger Verlag; 1986. p. 46-54.

Kahnert A, Hopken UE, Stein M, Bandermann S, Lipp M, Kaufmann SH. Mycobacterium tuberculosis triggers formation of lymphoid structure in murine lungs. The Journal of infectious diseases. 2007; 195:46–54. [PubMed: 17152008]

Kozakiewicz L, Phuah J, Flynn J, Chan J. The role of B cells and humoral immunity in Mycobacterium tuberculosis infection. Advances in experimental medicine and biology. 2013; 783:225–250. [PubMed: 23468112]

Machado LR, Bowdrey J, Ngaimisi E, Habtewold A, Minzi O, Makonnen E, Yimer G, Amogne W, Mugusi S, Janabi M, et al. Copy number variation of Fc gamma receptor genes in HIV-infected and HIV-tuberculosis co-infected individuals in sub-Saharan Africa. PloS one. 2013; 8:e78165. [PubMed: 24250791]

Maglione PJ, Xu J, Casadevall A, Chan J. Fc gamma receptors regulate immune activation and susceptibility during Mycobacterium tuberculosis infection. Journal of immunology. 2008; 180:3329–3338.

Maglione PJ, Xu J, Chan J. B cells moderate inflammatory progression and enhance bacterial containment upon pulmonary challenge with Mycobacterium tuberculosis. Journal of immunology. 2007; 178:7222–7234.

Mahan AE, Jennewein MF, Suscovich T, Dionne K, Tedesco J, Chung AW, Streeck H, Pau M, Schuitemaker H, Francis D, et al. Antigen-Specific Antibody Glycosylation Is Regulated via Vaccination. PLoS pathogens. 2016; 12:e1005456. [PubMed: 26982805]

Mahan AE, Tedesco J, Dionne K, Baruah K, Cheng HD, De Jager PL, Barouch DH, Suscovich T, Ackerman M, Crispin M, et al. A method for high-throughput, sensitive analysis of IgG Fc and Fab glycosylation by capillary electrophoresis. Journal of immunological methods. 2015; 417:34–44. [PubMed: 25523925]

Malhotra R, Wormald MR, Rudd PM, Fischer PB, Dwek RA, Sim RB. Glycosylation changes of IgG associated with rheumatoid arthritis can activate complement via the mannose-binding protein. Nat Med. 1995; 1:237–243. [PubMed: 7585040]

Martin CJ, Booty MG, Rosebrock TR, Nunes-Alves C, Desjardins DM, Keren I, Fortune SM, Remold HG, Behar SM. Efferocytosis is an innate antibacterial mechanism. Cell host & microbe. 2012; 12:289–300. [PubMed: 22980326]

Martinon F, Burns K, Tschopp J. The inflammasome: a molecular platform triggering activation of inflammatory caspases and processing of proIL-beta. Mol Cell. 2002; 10:417–426. [PubMed: 12191486]

McElvania Tekippe E, Allen IC, Hulseberg PD, Sullivan JT, McCann JR, Sandor M, Braunstein M, Ting JP. Granuloma formation and host defense in chronic Mycobacterium tuberculosis infection requires PYCARD/ASC but not NLRP3 or caspase-1. PloS one. 2010; 5:e12320. [PubMed: 20808838]

McEwan WA, Tam JC, Watkinson RE, Bidgood SR, Mallery DL, James LC. Intracellular antibody-bound pathogens stimulate immune signaling via the Fc receptor TRIM21. Nature immunology. 2013; 14:327–336. [PubMed: 23455675]

Mishra BB, Moura-Alves P, Sonawane A, Hacohen N, Griffiths G, Moita LF, Anes E. Mycobacterium tuberculosis protein ESAT-6 is a potent activator of the NLRP3/ASC inflammasome. Cellular microbiology. 2010; 12:1046–1063. [PubMed: 20148899]

Muller-Calleja N, Kohler A, Siebald B, Canisius A, Orning C, Radsak M, Stein P, Monnikes R, Lackner KJ. Cofactor-independent antiphospholipid antibodies activate the NLRP3-inflammasome via endosomal NADPH-oxidase: implications for the antiphospholipid syndrome. Thromb Haemost. 2015; 113:1071–1083. [PubMed: 25589411]

Nimmerjahn F, Ravetch JV. Fcgamma receptors as regulators of immune responses. Nature reviews Immunology. 2008; 8:34–47.

Niwa R, Natsume A, Uehara A, Wakitani M, Iida S, Uchida K, Satoh M, Shitara K. IgG subclass-independent improvement of antibody-dependent cellular cytotoxicity by fucose removal from Asn297-linked oligosaccharides. Journal of immunological methods. 2005; 306:151–160. [PubMed: 16219319]

Nunes-Alves C, Booty MG, Carpenter SM, Jayaraman P, Rothchild AC, Behar SM. In search of a new paradigm for protective immunity to TB. Nat Rev Microbiol. 2014; 12:289–299. [PubMed: 24590243]

O'Garra A, Redford PS, McNab FW, Bloom CI, Wilkinson RJ, Berry MP. The immune response in tuberculosis. Annual review of immunology. 2013; 31:475–527.

Olinger GG Jr, Pettitt J, Kim D, Working C, Bohorov O, Bratcher B, Hiatt E, Hume SD, Johnson AK, Morton J, et al. Delayed treatment of Ebola virus infection with plant-derived monoclonal antibodies provides protection in rhesus macaques. Proceedings of the National Academy of Sciences of the United States of America. 2012; 109:18030–18035. [PubMed: 23071322]

Olivares N, Marquina B, Mata-Espinoza D, Zatarain-Barron ZL, Pinzon CE, Estrada I, Parada C, Collin M, Rook G, Hernandez-Pando R. The protective effect of immunoglobulin in murine tuberculosis is dependent on IgG glycosylation. Pathogens and disease. 2013; 69:176–183. [PubMed: 23873753]

Parekh R, Isenberg D, Rook G, Roitt I, Dwek R, Rademacher T. A comparative analysis of disease-associated changes in the galactosylation of serum IgG. Journal of autoimmunity. 1989; 2:101–114.

Phuah J, Wong EA, Gideon HP, Maiello P, Coleman MT, Hendricks MR, Ruden R, Cirrincione LR, Chan J, Lin PL, et al. Effects of B Cell Depletion on Early Mycobacterium tuberculosis Infection in Cynomolgus Macaques. Infect Immun. 2016; 84:1301–1311. [PubMed: 26883591]

Phuah JY, Mattila JT, Lin PL, Flynn JL. Activated B cells in the granulomas of nonhuman primates infected with Mycobacterium tuberculosis. The American journal of pathology. 2012; 181:508–514. [PubMed: 22721647]

Pincetic A, Bournazos S, DiLillo DJ, Maamary J, Wang TT, Dahan R, Fiebiger BM, Ravetch JV. Type I and type II Fc receptors regulate innate and adaptive immunity. Nature immunology. 2014; 15:707–716. [PubMed: 25045879]

Pleass RJ. Fc-receptors and immunity to malaria: from models to vaccines. Parasite Immunol. 2009; 31:529–538. [PubMed: 19691552]

Pontillo A, Carvalho MS, Kamada AJ, Moura R, Schindler HC, Duarte AJ, Crovella S. Susceptibility to Mycobacterium tuberculosis infection in HIV-positive patients is associated with CARD8 genetic variant. J Acquir Immune Defic Syndr. 2013; 63:147–151. [PubMed: 23507658]

Prinz N, Clemens N, Strand D, Putz I, Lorenz M, Daiber A, Stein P, Degreif A, Radsak M, Schild H, et al. Antiphospholipid antibodies induce translocation of TLR7 and TLR8 to the endosome in human monocytes and plasmacytoid dendritic cells. Blood. 2011; 118:2322–2332. [PubMed: 21734241]

Raju TS. Terminal sugars of Fc glycans influence antibody effector functions of IgGs. Current opinion in immunology. 2008; 20:471–478. [PubMed: 18606225]

Ravetch JV, Perussia B. Alternative membrane forms of Fc gamma RIII(CD16) on human natural killer cells and neutrophils. Cell type-specific expression of two genes that differ in single nucleotide substitutions. J Exp Med. 1989; 170:481–497. [PubMed: 2526846]

Restrepo BI, Camerlin AJ, Rahbar MH, Wang W, Restrepo MA, Zarate I, Mora-Guzman F, Crespo-Solis JG, Briggs J, McCormick JB, et al. Cross-sectional assessment reveals high diabetes

prevalence among newly-diagnosed tuberculosis cases. Bulletin of the World Health Organization. 2011; 89:352–359. [PubMed: 21556303]

Schmaljohn A, Lewis GK. Cell-targeting antibodies in immunity to Ebola. Pathogens and disease. 2016; 74

Selman MH, de Jong SE, Soonawala D, Kroon FP, Adegnika AA, Deelder AM, Hokke CH, Yazdanbakhsh M, Wuhrer M. Changes in antigen-specific IgG1 Fc N-glycosylation upon influenza and tetanus vaccination. Mol Cell Proteomics. 2012; 11 M111 014563.

Steingart KR, Flores LL, Dendukuri N, Schiller I, Laal S, Ramsay A, Hopewell PC, Pai M. Commercial serological tests for the diagnosis of active pulmonary and extrapulmonary tuberculosis: an updated systematic review and meta-analysis. PLoS medicine. 2011; 8:e1001062. [PubMed: 21857806]

Suter E. Multiplication of tubercle bacilli within mononuclear phagocytes in tissue cultures derived from normal animals and animals vaccinated with BCG. J Exp Med. 1953; 97:235–245. [PubMed: 13022876]

Sutherland JS, Loxton AG, Haks MC, Kassa D, Ambrose L, Lee JS, Ran L, van Baarle D, Maertzdorf J, Howe R, et al. Differential gene expression of activating Fcgamma receptor classifies active tuberculosis regardless of human immunodeficiency virus status or ethnicity. Clinical microbiology and infection : the official publication of the European Society of Clinical Microbiology and Infectious Diseases. 2014; 20:O230–238.

Teitelbaum R, Glatman-Freedman A, Chen B, Robbins JB, Unanue E, Casadevall A, Bloom BR. A mAb recognizing a surface antigen of Mycobacterium tuberculosis enhances host survival. Proceedings of the National Academy of Sciences of the United States of America. 1998; 95:15688–15693. [PubMed: 9861031]

Tibshirani R. The lasso method for variable selection in the Cox model. Stat Med. 1997; 16:385–395. [PubMed: 9044528]

Torrado E, Fountain JJ, Robinson RT, Martino CA, Pearl JE, Rangel-Moreno J, Tighe M, Dunn R, Cooper AM. Differential and site specific impact of B cells in the protective immune response to Mycobacterium tuberculosis in the mouse. PloS one. 2013; 8:e61681. [PubMed: 23613902]

Tsai MC, Chakravarty S, Zhu G, Xu J, Tanaka K, Koch C, Tufariello J, Flynn J, Chan J. Characterization of the tuberculous granuloma in murine and human lungs: cellular composition and relative tissue oxygen tension. Cellular microbiology. 2006; 8:218–232. [PubMed: 16441433]

Ulrichs T, Kosmiadi GA, Trusov V, Jorg S, Pradl L, Titukhina M, Mishenko V, Gushina N, Kaufmann SH. Human tuberculous granulomas induce peripheral lymphoid follicle-like structures to orchestrate local host defence in the lung. J Pathol. 2004; 204:217–228. [PubMed: 15376257]

Vestrheim AC, Moen A, Egge-Jacobsen W, Reubsaet L, Halvorsen TG, Bratlie DB, Paulsen BS, Michaelsen TE. A pilot study showing differences in glycosylation patterns of IgG subclasses induced by pneumococcal, meningococcal, and two types of influenza vaccines. Immun Inflamm Dis. 2014; 2:76–91. [PubMed: 25400928]

Vidarsson G, Dekkers G, Rispens T. IgG subclasses and allotypes: from structure to effector functions. Frontiers in immunology. 2014; 5:520. [PubMed: 25368619]

Vordermeier HM, Venkataprasad N, Harris DP, Ivanyi J. Increase of tuberculous infection in the organs of B cell-deficient mice. Clinical and experimental immunology. 1996; 106:312–316. [PubMed: 8918578]

Zak DE, Penn-Nicholson A, Scriba TJ, Thompson E, Suliman S, Amon LM, Mahomed H, Erasmus M, Whatney W, Hussey GD, et al. A blood RNA signature for tuberculosis disease risk: a prospective cohort study. Lancet. 2016; 387:2312–2322. [PubMed: 27017310]

Zimmerli S, Edwards S, Ernst JD. Selective receptor blockade during phagocytosis does not alter the survival and growth of Mycobacterium tuberculosis in human macrophages. Am J Respir Cell Mol Biol. 1996; 15:760–770. [PubMed: 8969271]

Zou G, Ochiai H, Huang W, Yang Q, Li C, Wang LX. Chemoenzymatic synthesis and Fcgamma receptor binding of homogeneous glycoforms of antibody Fc domain. Presence of a bisecting sugar moiety enhances the affinity of Fc to FcgammaIIIa receptor. Journal of the American Chemical Society. 2011; 133:18975–18991. [PubMed: 22004528]

Zumla A, Raviglione M, Hafner R, von Reyn CF. Tuberculosis. The New England journal of medicine. 2013; 368:745–755. [PubMed: 23425167]

Highlights

- Individuals with latent and active TB infection have divergent humoral signatures.
- Antibodies in latent TB infection have enhanced Fc effector profiles.
- Antibody glycosylation patterns can discriminate between latent and active TB.
- Antibodies in latent TB infection drive macrophages to kill intracellular bacteria.

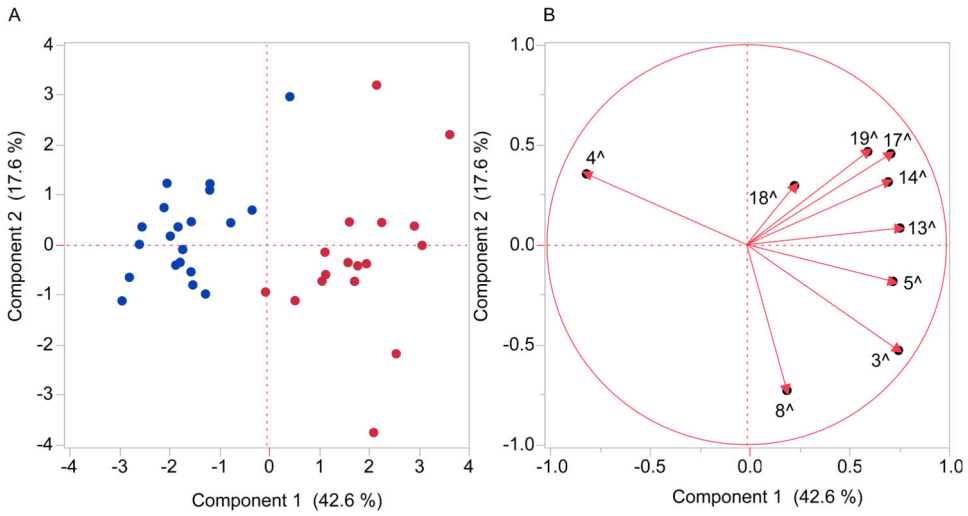

Figure 1. Individuals with Ltb and Atb exhibit divergent humoral profiles

A least absolute shrinkage and selection operator (LASSO) (Tibshirani, 1997) identified nine Ab features (^ in Table 2) from the original 69 that best discriminate Ltb from Atb humoral profiles. Principal component analysis (PCA) using these nine features alone demonstrates the (A) dot plot of nearly non-overlapping Ab profiles in Ltb (n=22, blue) compared to Atb (n=20, red) individuals. The nine Ab features are represented in the Loadings Plot (B), a mirror image of the PCA dot plot, where the location of the Ab features reflects the distribution of the individuals in the dot plot (A).

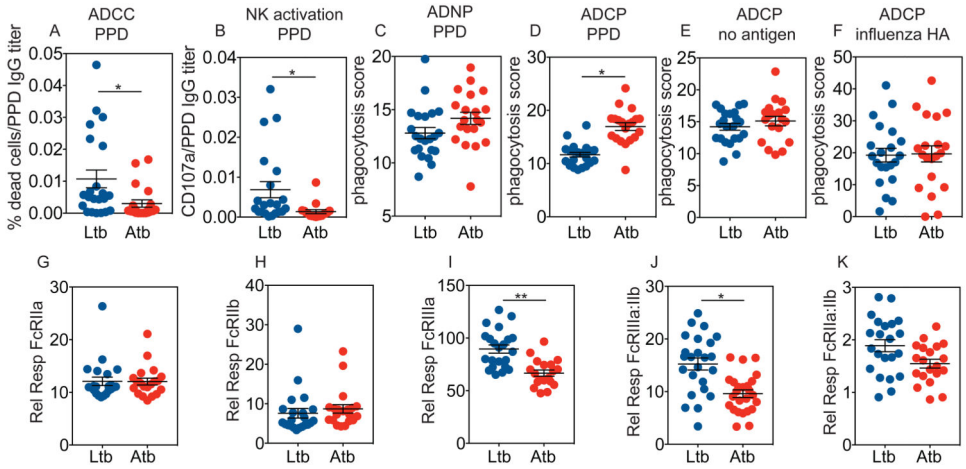

Figure 2. Abs from Ltb and Atb individuals exhibit distinct Fc effector functional profiles

IgG purified from the serum of individuals with Ltb (n=22) and Atb (n=20) was assayed for its ability to mediate Fc effector functions including ADCC (A), Ab-dependent NK cell activation (B), Ab-dependent neutrophil phagocytosis (ADNP), (C) Ab-dependent cellular phagocytosis by THP1 monocytes (D), phagocytosis of uncoated beads by THP1 monocytes (E), and phagocytosis of influenza HA-coated beads (F) by THP1 monocytes. Functional differences were not due to endotoxin levels (Supplemental Figure 2L). Binding of polyclonal IgG to (G) FcγRIIa, (H) FcγRIIb, and (I) FcγRIIIa was evaluated by surface plasmon resonance. Integrated ratios of binding are plotted in (J) FcγRIIIa:FcγRIIb and (K) FcγRIIa:FcγRIIb. The error bars represent mean ± SEM of the individuals. p values were calculated using Mann Whitney tests and adjusted for age and sex. All experiments were run in triplicate. * p≤0.05; ** p≤0.01.

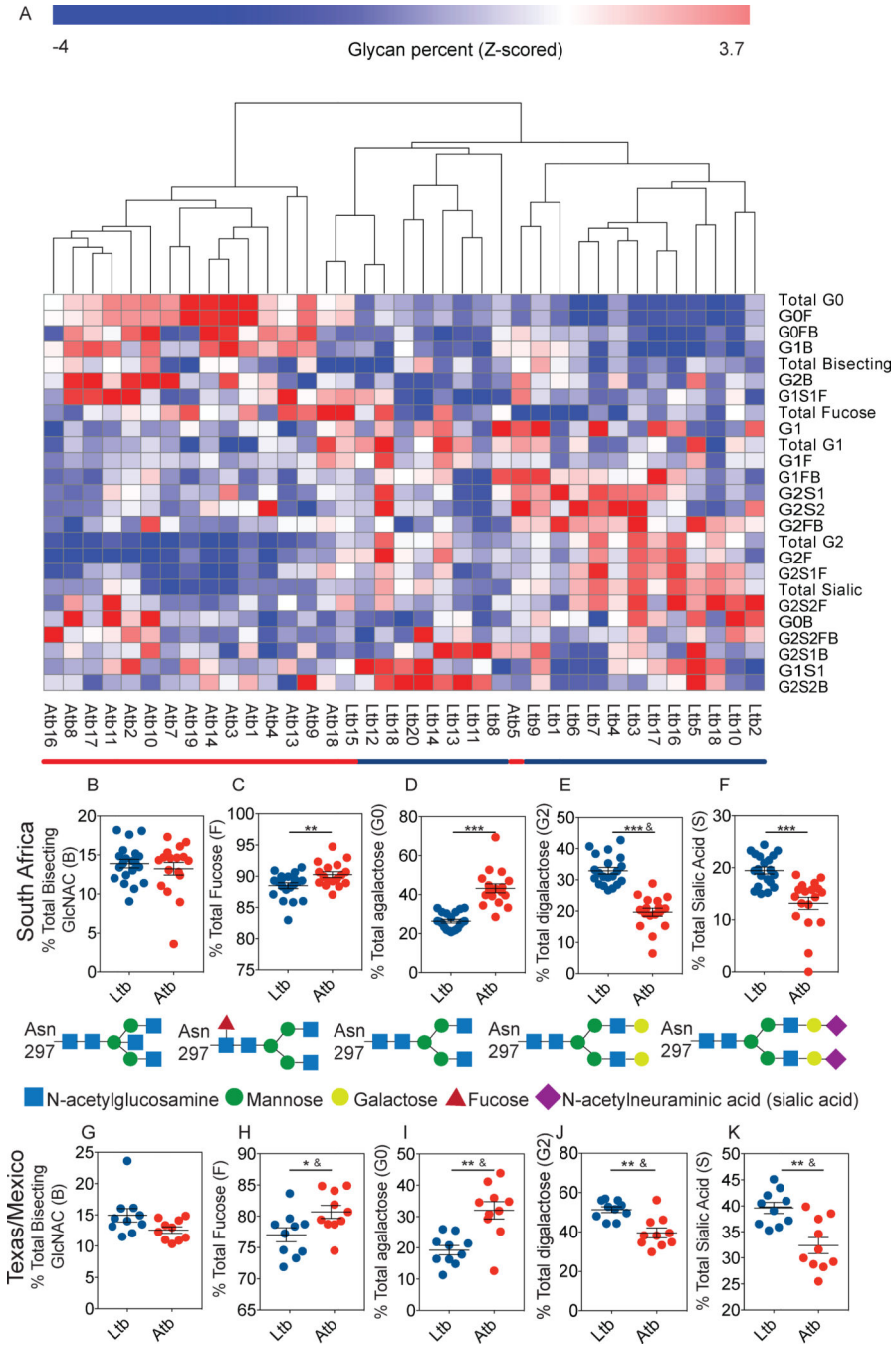

Figure 3. Abs are differentially glycosylated in individuals with Ltb and Atb

The heatmap illustrates the unsupervised clustering using one minus Pearson correlation of the Ab glycan profiles of Ltb (n=20, blue) and Atb (n=16, red) individuals from South Africa (A). Glycan structures are represented on the y-axis as the percent of all glycoform variants (z-scored). Dot plots represent differences between Ltb and Atb with respect to the major glycan categories: bisecting N-acetylglycosamine (GlcNAC-B: all structures containing a bisecting GlcNAc) (B and G), fucose (F: all structures containing fucose) (C and H), agalactosylated structures (G0: all structures lacking galactose) (D and I),

digalactosylated structures (G2: all structures containing two galactose structures) (E and J), and sialylated structures (S: all structures with at least one sialic acid) (F and K). Corresponding diagrammatic representation of the common N-linked glycans quantified are shown. Dot plots in (B-F) derive from individuals from South Africa. Dot plots in (G-K) derive from individuals with Ltb (n=10) and Atb (n=10) from Texas/Mexico. Bars show mean of individuals ± SEM. p values were calculated using Mann Whitney tests, adjusted for age and sex, with a post-hoc Holms correction (Holm, 1979). & denotes the glycan features that remained significant following Holms correction. * $p \leq 0.05$; ** $p \leq 0.01$; *** $p \leq 0.001$.

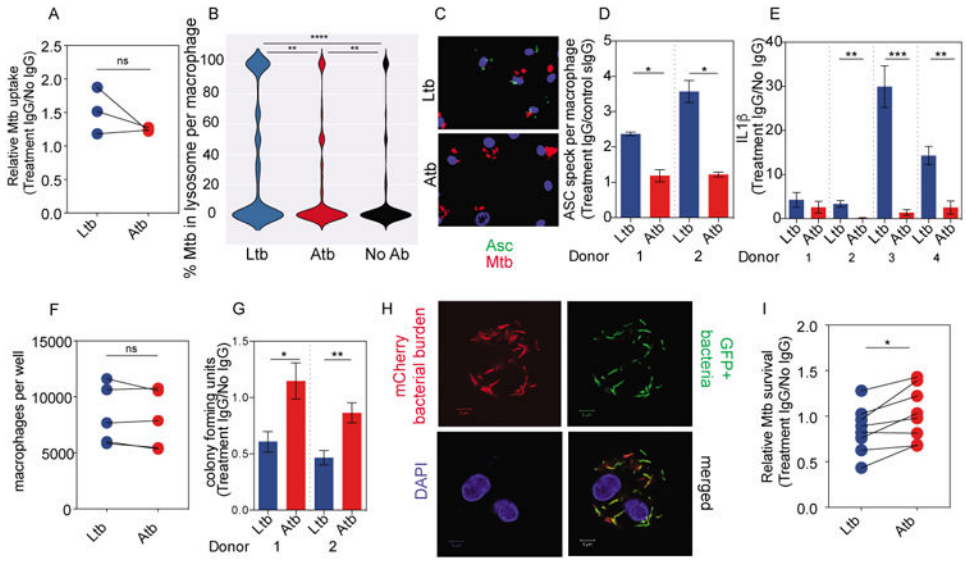

Figure 4. Ltb compared to Atb Abs enhance macrophage activation and intracellular Mtb restriction

The dot plot represents Mtb uptake following Ltb or Atb Ab treatment compared to the no Ab control, with lines linking results from the same macrophage donor (A). Violin plots show the distribution of percent co-localization of bacteria within lysosomes measured in 200–600 macrophages per well (B). Representative ASC staining demonstrating the formation of perinuclear structure ASC specks (green) and Mtb (red) in the presence of Ltb Abs (C). ASC-speck numbers were quantified in 200–600 macrophages per well as a ratio to control non-specific pooled seronegative immunoglobulin (D). Inflammasome activity was further examined by IL1β release by ELISA following Mtb-infected macrophage treatment with Ltb or Atb Abs (E). Macrophage numbers were quantified by DAPI enumeration (F). Bacterial burden was ascertained by colony forming units in sextuplicate (G). Representative confocal microscopy panels show, following anhydrotetracycline induction of GFP expression in transcriptionally active bacteria, the constitutive mCherry fluorophore marking total bacterial burden and a GFP+ bacterial subpopulation within macrophages (DAPI) (H). Bacterial survival is plotted in the dot plot ($live_{GFP}/total_{MCH}$) in Mtb-infected macrophages derived from eight different macrophage donors. Lines depict comparison between same donor macrophages (I). Differences were not due to endotoxin levels (Supplemental Figure 2L and 5D). Wilcoxon matched-pairs signed rank (A, F and I), student t (D, E and G) and Mann Whitney (B) tests were used to calculate p values. Bars represent the mean of technical replicates ± SEM. * $p \leq 0.05$; ** $p \leq 0.01$; *** $p \leq 0.001$; ns= not significant.

Table 1

Demographic characteristics in cohorts from South Africa and Texas/Mexico.

South Africa	**Latent TB**	**Active TB**
Total number	22	20
Female	15	5
Male	7	15
Age	26 (21.75-35.50)	38 (30.00-51.75)
Sputum smear	0	2 (1-3)
Treatment days	0	5 (2-6)
Texas/Mexico		
Total number	10	10
Female	5	5
Male	5	5
Age	35 (26.25-42.50)	24.50 (18.75-32.00)
Sputum smear	n/a	n/a
Treatment days	0	0

Median and interquartile ranges (IQR) are shown.

n/a marks data that are unavailable.

Table 2

Ab features that differ between Ltb and Atb *(South Africa)*.

The Ab features listed in this table are those that remained statistically significant ($p<0.05$) after adjustment for age and sex using a robust regression model on the 69 Ab features with individual measurements sufficient for regression analysis.

	Antibody feature	P value adjusted for age and sex
1[&]	Total G2	0.0002
2	G0F	0.0003
3[^]	Total G0	0.0003
4[^]	G2F	0.0005
5[^]	PPD ADCP	0.001
6	Total DiSialic Acid	0.001
7	FcR3a binding	0.002
8[^]	Total Fucose	0.0041
9	G1FB	0.0053
10	G2S2	0.0081
11	G2S1F	0.0082
12	Cytosol protein ADCP	0.01
13[^]	Culture filtrate ADCP	0.01
14[^]	Cell membrane ADCP	0.01
15	G2S1	0.0145
16	FcR3a2b binding	0.0174
17[^]	Soluble protein ADCP	0.02
18[^]	G1S1F	0.0385
19[^]	Soluble protein IgG1	0.04

[&] statistically significant after correction for multiple comparisons (Holm, 1979)

[^] identified following parallel multivariate feature reduction analysis using LASSO (Tibshirani, 1997), used in principal component analysis (Jolliffe, 1986) (Figure 1).

Table 3

Ab features that differ between Ltb and Atb *(Texas).*

	Antibody feature	P value adjusted for age and sex
1[&]	Total G2	0.003
2[&]	Total G0	0.004
3[&]	Total sialic acid	0.009
4[&]	Total fucose	0.025
5	Total bisecting GlcNAC	0.159

[&] statistically significant after correction for multiple comparisons (Holm, 1979)